This document is published in:

Combustion and Flame, Vol. 160, nº 1, pp. 76-82

DOI: http://dx.doi.org/10.1016/j.combustflame.2012.09.014

Four-step and three-step systematically reduced chemistry for wide-range H_2–air combustion problems

Pierre Boivin [a,1], Antonio L. Sánchez [b,a,*], Forman A. Williams [b]

[a] Dept. Ingeniería Térmica y de Fluidos, Universidad Carlos III de Madrid, Leganés 28911, Spain
[b] Dept. of Mechanical and Aerospace Engineering, University of California San Diego, La Jolla, CA 92093-0411, USA

A B S T R A C T

The feasibility of developing multipurpose reduced chemistry that is able to describe, with sufficient accuracy, premixed and non-premixed flames, one-dimensional detonations, high-temperature autoignition, and also low-temperature autoignition is explored. A four-step mechanism with O and OH in steady state is thoroughly tested and is shown to give satisfactory results under all conditions. The possibility of reducing this to a three-step mechanism, to decrease computation times without compromising the range of applicability is then investigated. The originality of this work resides in introducing a single species X, representing either HO_2 for high-temperature ignition or H_2O_2 for low-temperature ignition. An algorithm is defined that covers the entire range without significant degradation of accuracy. Integrations show promising results for different laminar test cases, and applicability to turbulent flows is indicated.

Keywords:
Autoignition
Reduced chemistry
Hydrogen

1. Introduction

Systematic reduction of hydrogen–oxygen chemistry is helpful for speeding computations of multidimensional and turbulent combustion problems. For this reason, there have been a number of earlier investigations of reduced chemistry for hydrogen [1–3]. Previous studies have found, for example, that there exists a two-step description that is sufficiently accurate for most purposes in describing laminar deflagrations and diffusion flames, but that a different description is needed for autoignition processes. In our previous work [4], which may be consulted for further background, we have developed a three-step reduced-chemistry description that encompasses both flames and autoignition processes that occur above the pressure-dependent crossover temperature T_c of the $H + O_2 \rightarrow OH + H$ branching step and the $H + O_2 + M \rightarrow HO_2 + M$ recombination step, which define the second explosion limit, of interest, for example, in supersonic combustion. The procedure involved chain-branching reaction-rate modifications, based on analytical ignition-time studies, keyed to switch on when HO_2 departed sufficiently from its steady-state, to account for the fact that O and OH do not maintain steady states in high-temperature autoignition. While the procedure was shown [4] to work well for the intended range of conditions, it cannot apply to low-temperature autoignition, below crossover, for which suitable reduced chemistry is different [5,6]. The present contribution addresses extending the previous [4] approach to include, as well, the low-temperature autoignition, a regime of interest in applications involving gas-turbine combustion.

The three-step reduced mechanism [4] is derived from a subset of 12 elementary reactions, selected from the full set of 21 reactions, listed in Table 1, where the rate parameters given are those of the detailed San Diego mechanism [7]. The three-step mechanism has been validated in both laminar [4] and turbulent [8] contexts, both for flames (premixed and non-premixed) and autoignition above the second explosion limit.

Figure 1 compares ignition-time predictions obtained from detailed chemistry with those obtained using different reduced-chemistry descriptions, including, in particular, the three-step scheme derived in [4]. Predictions with the short 12-step chemistry are not shown in the figure because the resulting curve could not be distinguished from that of the 21-step chemistry. As can be seen, our previous three-step chemistry yields excellent agreement with predictions of detailed chemistry for conditions above the second explosion limit, the location of which is indicated in the figure by a vertical line, but it is unable to reproduce with good accuracy autoignition histories close or below the second explosion limit, where departures increase as the temperature decreases. The other curves in this figure are to be discussed later.

The inaccuracies in treating autoignition below the second explosion limit by our previous [4] reduced chemistry are not related to the choice of the 12-reaction subset upon which the

* Corresponding author at: Dept. Ingeniería Térmica y de Fluidos, Universidad Carlos III de Madrid, Leganés 28911, Spain. Tel.: +34 91 6249950; fax: +34 91 6249430.
E-mail address: asanchez@ing.uc3m.es (A.L. Sánchez).
[1] Present address: Dept. of Combustion, Space Propulsion Division, Snecma, Vernon, France.

Table 1
Rate coefficients in Arrhenius form $k = AT^n \exp(-E/R^oT)$, for the skeletal mechanism.

	Reaction		A[a]	n	E[a]		A[a]	n	E[a]
1	$H + O_2 \rightleftharpoons OH + O$	k_f	3.52×10^{16}	−0.7	71.42	k_b	7.04×10^{13}	−0.26	0.60
2	$H_2 + O \rightleftharpoons OH + H$	k_f	5.06×10^{4}	2.67	26.32	k_b	3.03×10^{4}	2.63	20.23
3	$H_2 + OH \rightleftharpoons H_2O + H$	k_f	1.17×10^{9}	1.3	15.21	k_b	1.28×10^{10}	1.19	78.25
4	$H + O_2 + M \rightharpoonup HO_2 + M$[b]	k_0	5.75×10^{19}	−1.4	0.0	k_∞	4.65×10^{12}	0.44	0.0
5	$HO_2 + H \rightharpoonup 2OH$		7.08×10^{13}	0.0	1.23				
6	$HO_2 + H \rightleftharpoons H_2 + O_2$	k_f	1.66×10^{13}	0.0	3.44	k_b	2.69×10^{12}	0.36	231.86
7	$HO_2 + OH \rightharpoonup H_2O + O_2$		2.89×10^{13}	0.0	−2.08				
8	$H + OH + M \rightleftharpoons H_2O + M$[c]	k_f	4.00×10^{22}	−2.0	0.0	k_b	1.03×10^{23}	−1.75	496.14
9	$2H + M \rightleftharpoons H_2 + M$[c]	k_f	1.30×10^{18}	−1.0	0.0	k_b	3.04×10^{17}	−0.65	433.09
10	$2HO_2 \rightharpoonup H_2O_2 + O_2$		3.02×10^{12}	0.0	5.8				
11	$HO_2 + H_2 \rightharpoonup H_2O_2 + H$		1.62×10^{11}	0.61	100.14				
12	$H_2O_2 + M \rightharpoonup 2OH + M$[d]	k_0	8.15×10^{23}	−1.9	207.62	k_∞	2.62×10^{19}	−1.39	214.74

[a] Units are mol, s, cm^3, kJ, and K.
[b] Chaperon efficiencies are 2.5 for H_2, 16.0 for H_2O, and 1.0 for all other species; Troe falloff with $F_c = 0.5$.
[c] Chaperon efficiencies are 2.5 for H_2, 12.0 for H_2O, and 1.0 for all other species.
[d] Chaperon efficiencies are 2.5 for H_2, 6.0 for H_2O, and 1.0 for all other species; $F_c = 0.265\exp(-T/94\ \mathrm{K}) + 0.735\exp(-T/1756\ \mathrm{K}) + \exp(-5182\ \mathrm{K}/T)$.

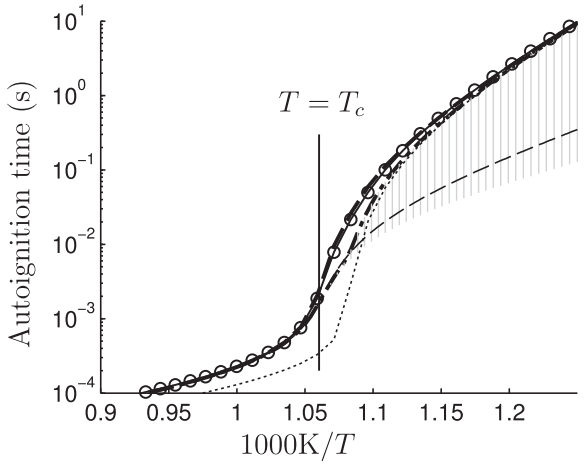

Fig. 1. The isobaric temperature-inflection ignition time at atmospheric pressure as obtained for a stoichiometric H_2–air mixture by numerical integration of the conservation equations with the detailed 21-step chemistry (solid curve and circles), with the 3-step reduced mechanism making use of the high-temperature set of rates with the branching modification (light dashed curve), with the 3-step low-temperature set of rates (dotted curve), with the 4-step reduced chemistry including both HO_2 and H_2O_2 (heavy dashed curve), and with the hybrid description (heavy dash-dotted curve). The gray bars shade the region where use is made of the low-temperature set of rates in the hybrid scheme.

reduction is built, but rather they are a consequence of the species assumed to be in steady state in this description. Only eight elementary reactions have to be considered to accurately describe the low-temperature autoignition regime [5,6,9], and each of them (resp. 1*f*, 2*f*, 3*f*, 4*f*, 6*b*, 10*f*, 11*f*, 12*f*) is included in the subset of 12 reactions considered here. We shall see below that modifications to the chemistry, guided by knowledge gained in [6], can lead to derivations of reduced descriptions that can successfully describe not only flames and high-temperature autoignition, but also autoignition events below the second explosion limit.

2. The four-step reduced-chemistry mechanism

As seen in [6], while the H_2O_2 steady state is an excellent assumption for flames and also during high-temperature autoignition, it is, however, never a valid approximation during the thermal-runaway events that characterize autoignition below crossover. It then seems natural, in searching to extend the range of validity of the reduced chemistry, to consider the four-step reduced mechanism that follows from assuming that only O and OH are in steady state, while H, HO_2 and H_2O_2 are not. Starting from the 12 chemical steps in Table 1, and linearly combining the production rates $\dot{C}_i$ of each species i yields

$$\begin{aligned}
&\dot{C}_{H_2} - \dot{C}_{OH} - 2\dot{C}_O = -3\omega_I + \omega_{II} - \omega_{III} - \omega_{IV},\\
&\dot{C}_{O_2} = -\omega_I - \omega_{III} - \omega_{IV},\\
&\dot{C}_{H_2O} + \dot{C}_O + \dot{C}_{OH} = 2\omega_I,\\
&\dot{C}_H + \dot{C}_{OH} + 2\dot{C}_O = 2\omega_I - 2\omega_{II} + \omega_{III},\\
&\dot{C}_{HO_2} = \omega_{III},\\
&\dot{C}_{H_2O_2} = \omega_{IV},
\end{aligned} \tag{1}$$

where

$$\begin{aligned}
\omega_I &= \omega_1 + \omega_{5f} + \omega_{12f},\\
\omega_{II} &= \omega_{4f} + \omega_8 + \omega_9 - \omega_{10f} - \omega_{11f},\\
\omega_{III} &= \omega_{4f} - \omega_{5f} - \omega_6 - \omega_{7f} - 2\omega_{10f} - \omega_{11f},\\
\omega_{IV} &= \omega_{10f} + \omega_{11f} - \omega_{12f}.
\end{aligned} \tag{2}$$

Neglecting in (1) the small concentrations of the steady-state species O and OH reveals that the previous system of equations corresponds to the four overall reactions

$$\begin{aligned}
&3H_2 + O_2 \overset{I}{\rightleftharpoons} 2H_2O + 2H,\\
&H + H + M \overset{II}{\rightleftharpoons} H_2 + M,\\
&H_2 + O_2 \overset{III}{\rightleftharpoons} HO_2 + H,\\
&H_2 + O_2 \overset{IV}{\rightleftharpoons} H_2O_2.
\end{aligned} \tag{3}$$

The relevance of the first two of these to flames has been explained previously [1], and the importance of the third in high temperature autoignition has been described [4], while the mathematically convenient fourth step, combined with the first and third, reflects the low-temperature net radical production through H_2O_2[6,5]. The computation of the rates ω_{1b}, ω_{7f} and ω_{8f} requires knowledge of the concentrations of O and OH, which can be obtained in explicit form by solving their steady-state equations. The expression for C_O given in [4] remains valid, whereas the expression for C_{OH} must be modified to account for the fact that H_2O_2 is not assumed to be in steady state, yielding

$$C_{OH} = [(A_1^2 + 4A_0A_2)^{1/2} - A_1]/(2A_2), \tag{4}$$

$$C_O = \frac{k_{1f}C_HC_{O_2} + k_{2b}C_{OH}C_H}{k_{1b}C_{OH} + k_{2f}C_{H_2}}, \tag{5}$$

where

$$A_0 = C_{H_2} k_{2f} (2k_{1f} C_H C_{O_2} + k_{3b} C_H C_{H_2O} + 2k_{5f} C_H C_{HO_2} + 2k_{12f} C_{H_2O_2} C_{M_{12}} + k_{8b} C_{M_8} C_{H_2O}),$$

$$A_1 = +C_{H_2} k_{2f} (k_{8f} C_{M_8} C_H + k_{7f} C_{HO_2} + k_{3f} C_{H_2}) - k_{1b} (k_{3b} C_H C_{H_2O} + 2k_{5f} C_H C_{HO_2} + 2k_{12f} C_{H_2O_2} C_{M_{12}} + k_{8b} C_{M_8} C_{H_2O}), \quad (6)$$

$$A_2 = k_{1b} (2k_{2b} C_H + k_{3f} C_{H_2} + k_{7f} C_{HO_2} + k_{8f} C_{M_8} C_H).$$

To account for the O and OH departures from steady states found during high-temperature autoignition events, the four overall rates are to be modified wherever HO_2 is not in steady-state, following the procedure presented in [4]. The accuracy of the resulting four-step description is illustrated by the heavy dashed curve in Fig. 1, which shows the resulting predictions of ignition times. The agreement with predictions of the detailed mechanism is seen to be excellent. In addition, for flames, in which HO_2 and H_2O_2 steady-state approximations are good, this mechanism reduces to the two-step mechanism given below in (10), thus resulting in comparable accuracy. This four-step mechanism therefore clearly spans the entire range.

3. The two separate three-step mechanisms for autoignition

According to the discussions given in [4,6,5], simplified versions of this four-step reduced mechanism apply for ignition conditions away from the second explosion limit. Thus, for ignition above crossover, H_2O_2 may be assumed to be in steady state, leading to the three-step reduced chemistry

$$\begin{aligned} &3H_2 + O_2 \overset{\text{I}}{\rightleftharpoons} 2H_2O + 2H, \\ &H + H + M \overset{\text{II}}{\rightleftharpoons} H_2 + M, \\ &H_2 + O_2 \overset{\text{III}}{\rightleftharpoons} HO_2 + H \end{aligned} \quad (7)$$

derived in [4]. On the other hand, for conditions sufficiently below the second explosion limit, the results presented in [6] suggest that the HO_2 steady-state assumption is a reasonable approximation, whereas that of H_2O_2 is not. Introducing a steady-state approximation for HO_2 reduces the four-step chemistry to

$$\begin{aligned} &3H_2 + O_2 \overset{\text{I}}{\rightleftharpoons} 2H_2O + 2H \\ &H + H + M \overset{\text{II}}{\rightleftharpoons} H_2 + M \\ &H_2 + O_2 \overset{\text{IV}}{\rightleftharpoons} H_2O_2, \end{aligned} \quad (8)$$

with corresponding rates given in (2). For evaluation of elementary rates, the concentrations of the steady-state species OH and O are computed from (4) and (5), whereas that of HO_2 is evaluated from

$$\begin{aligned} &C_{HO_2} = (B_2^2 + B_1)^{1/2} - B_2, \\ &B_1 = (k_{6b} C_{H_2} C_{O_2} + k_{4f} C_H C_{O_2} C_{M_4})/(2k_{10f}), \\ &B_2 = (k_{5f} C_H + k_{6f} C_H + k_{7f} C_{OH} + k_{11f} C_{H_2})/(4k_{10f}). \end{aligned} \quad (9)$$

As can be seen in the comparisons of Fig. 1, while a four-step mechanism including both HO_2 and H_2O_2 gives accurate predictions for ignition times regardless of the initial temperature, the two separate three-step descriptions derived by considering either H and HO_2 or H and H_2O_2 to be out of steady state, the light dashed curve and the dotted curve, give reasonable accuracy in their expected ranges of validity, but are much less accurate otherwise.

Note that for flames, where HO_2 and H_2O_2 may be additionally assumed to be in steady state [1,10,11], both three-step descriptions naturally reduce to a single two-step reduced mechanism

$$\begin{aligned} &3H_2 + O_2 \overset{\text{I}}{\rightleftharpoons} 2H_2O + 2H \\ &H + H + M \overset{\text{II}}{\rightleftharpoons} H_2 + M \end{aligned} \quad (10)$$

with rates

$$\begin{aligned} &\omega_{\text{I}} = \omega_1 + \omega_{5f} + \omega_{10f} + \omega_{11f} \\ &\omega_{\text{II}} = \omega_{4f} + \omega_8 + \omega_9 - \omega_{10f} - \omega_{11f}, \end{aligned} \quad (11)$$

which is an extension to that introduced in [1] (in particular including reaction 10*f*, 11*f*, and implicitly 12*f*, important for high-pressure conditions) that provides sufficient accuracy for laminar burning velocities and strain rates at extinction. If there is interest in autoignition, however, then the two-step mechanism is not sufficient, and either HO_2 or H_2O_2 needs to be incorporated in the reduced chemistry as an additional chemical species out of steady state, the selection of one or the other depending on whether or not the temperature is above crossover. These two species are hardly ever simultaneously far out of steady state, the only exception being ignition events at temperatures close to crossover, while for all other combustion situations the steady-state assumption is accurate for at least one of these two species. This observation motivates the investigation given below, in which a three-step mechanism is proposed as the minimum description able to encompass all combustion processes. Besides H atoms, a second species out of steady state, a surrogate intermediate X, is introduced to represent the role of either HO_2 or H_2O_2, depending on the local conditions.

4. A universal three-step description

In defining the properties of the surrogate X one may take into account the fact that, since in low-temperature autoignition the contribution of the H_2O_2 enthalpy is negligible for obtaining the correct induction time, as shown in [6], it is possible, with no adverse consequences, to select the enthalpy of formation of X to be equal to that of HO_2. On the other hand, given that the two molecules H_2O_2 and HO_2 have similar transport properties, predictions are quite independent of which diffusivity is employed for X, with that of HO_2 used in the computations below. The main difficulties in the development stem from the fact that the overall reactions for the consumption of HO_2 and H_2O_2 are different, with reaction III involving H-atom production, while reaction IV does not. Besides, since the expressions for the two sets of overall rates are different, a local criterion must be introduced to decide which one of the two sets of reactions is to be employed.

4.1. Modified reaction rates

In the development, let us consider the three overall steps

$$\begin{aligned} &3H_2 + O_2 \overset{\text{I}}{\rightleftharpoons} 2H_2O + 2H \\ &H + H + M \overset{\text{II}}{\rightleftharpoons} H_2 + M \\ &H_2 + O_2 \overset{\text{III}}{\rightleftharpoons} X + H, \end{aligned} \quad (12)$$

which are exactly those for high-temperature ignition, with X = HO_2 and with overall rates given in [4]:

$$\begin{aligned} &\omega_{\text{I}}^{+} = \omega_1 + \omega_{5f} + \omega_{10f} + \omega_{11f} \\ &\omega_{\text{II}}^{+} = \omega_{4f} + \omega_8 + \omega_9 - \omega_{10f} - \omega_{11f} \\ &\omega_{\text{III}}^{+} = \omega_{4f} - \omega_{5f} - \omega_6 - \omega_{7f} - 2\omega_{10f} - \omega_{11f}, \end{aligned} \quad (13)$$

to be corrected as in [4] in places where X (HO_2, in this case) is out of steady state.

As previously noted, an incorrect H-atom production rate would follow from using the above overall reaction III given in (12) with X = H_2O_2 for describing low-temperature ignition, because this reaction produces H atoms, while the overall reaction IV does not. This difficulty can be avoided by modifying the rate of II according to $\omega_{\text{II}}^{-} = \omega_{\text{II}} + \omega_{\text{IV}}/2$, resulting finally in the overall rate expressions

$$\begin{aligned}\omega_{\rm I}^{-} &= \omega_{\rm I} = \omega_1 + \omega_{5f} + \omega_{12f}\\ \omega_{\rm II}^{-} &= \omega_{\rm II} + \omega_{\rm IV}/2\\ &= \omega_{4f} + \omega_8 + \omega_9 - (\omega_{10f} + \omega_{11f} + \omega_{12f})/2\\ \omega_{\rm III}^{-} &= \omega_{\rm IV} = \omega_{10f} + \omega_{11f} - \omega_{12f},\end{aligned} \tag{14}$$

for describing low-temperature ignition with (12). The resulting rate expression for H is then the same as that corresponding to (8) and appearing in (2). Clearly, the modification proposed introduces errors in H_2 production, but these errors are unimportant for ignition, because reactant consumption is negligible prior to the thermal runaway. As a result, the ignition times obtained with the three-step mechanism defined in (8) with the overall rates (2), turn out to be indistinguishable from those obtained with the mechanism (12) with overall rates (14).

Computations of flames with the three overall steps (12) give almost identical results when the two different set or rates (13) and (14) are employed because for flames the intermediate X is always in steady state, so that both mechanisms effectively reduce to the same two-step mechanism (10). This is illustrated in Fig. 2, which compares laminar burning velocities obtained with the mechanism (12) for the two sets of rates with those obtained with detailed chemistry. The differences seen in Fig. 2 in the vicinity of stoichiometric conditions for the lower pressure are due primarily to inaccuracies in the steady-state approximations for O and OH and are acceptable for most purposes, as has been discussed previously [4].

4.2. Criterion for selection of overall rates

The three overall steps displayed in (12) involve two chemical intermediates X and H. Two different sets of rates, given in (13) and (14), are found to apply depending on the combustion conditions. The results in Fig. 2 suggest that we may focus on autoignition alone in seeking a criterion to decide which one of the two sets of overall rates applies, since the selection is inconsequential for flame descriptions. In general, one wishes to use (13) when high-temperature ignition is occurring and (14) when low-temperature ignition is occurring, but a computational criterion is needed to enforce the choice.

To identify places where the rates (14) apply, an obvious choice is to simply evaluate whether the local temperature is below crossover. This criterion is poor, however, in that it leads to severe disparities in resulting ignition times in neighboring points of the flow field as the conditions vary from slightly above to slightly below crossover (see the homogeneous ignition results given in Fig. 1). As an alternative, the selection criterion may take advantage of the observation, made in [6], that during low-temperature autoignition processes, H radicals are found to be in steady state after a short initial period of radical build up, whereas this species remains always out of steady state during high-temperature autoignition. A better criterion, then, may be to use (14) when H is in steady state.

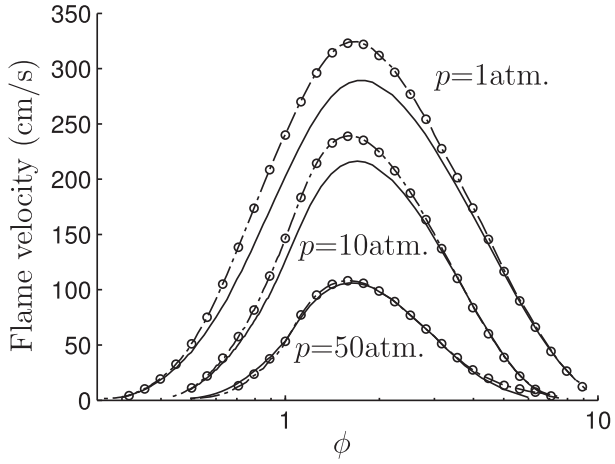

Fig. 2. The variation with equivalence ratio of the laminar burning velocity of hydrogen–air planar atmospheric deflagrations with initial temperature T_u = 300 K as obtained with the detailed 21-step chemistry (solid curves), with the 3-step chemistry (12) with overall rates $\omega^{+}_{\rm I,II,III}$ (dashed-dotted curves) and with overall rates $\omega^{-}_{\rm I,II,III}$ (symbols).

To evaluate the steady state for H atoms, reactions important in low-temperature ignition are used to write the production rate

$$\omega_P = \omega_{6b} + \omega_{11f} + 2\omega_{12f} + 2\omega_{1f} \tag{15}$$

and the consumption rate

$$\omega_C = \omega_{4f}, \tag{16}$$

so that the net chemical production rate is found as the difference, $\dot{C}_{\rm H} = \omega_P - \omega_C$. The reaction rate ω_{12f} appearing in (15) may be evaluated as $k_{12f}C_{\rm X}C_{\rm M_{12}}$, since X is H_2O_2 under these conditions, whereas the HO_2 concentration, needed for computing ω_{11f}, is obtained from the steady-state expression

$$C_{\rm HO_2} = \frac{k_{11f}C_{\rm H_2}\alpha/(1-\alpha) + \sqrt{k_{11f}^2 C_{\rm H_2}^2 \alpha^2/(1-\alpha)^2 + 8k_{10f}k_{6b}(2-\alpha)/(1-\alpha)}}{2k_{10f}}, \tag{17}$$

with $\alpha = 2k_{1f}/(k_{4f}C_{\rm M_4})$, which, unlike in [6], includes the rate of the elementary reaction 11*f*, for increased accuracy near crossover.

The condition $(\omega_P - \omega_C) \ll \omega_P$, satisfied in places where the H atom is in steady state, can be based on a small threshold value ε, such that if $(\omega_P - \omega_C)/\omega_P < \varepsilon$ the rates (14) should be used, whereas (13) applies otherwise. Using the elementary rates above to rewrite $(\omega_P - \omega_C)/\omega_P < \varepsilon$ leads to a condition on the concentration of H atoms,

$$C_{\rm H}[(1+\varepsilon)k_{4f}C_{\rm M_4} - 2k_{1f}]C_{\rm O_2} > k_{6b}C_{\rm H_2}C_{\rm O_2} + k_{11f}C_{\rm H_2}C_{\rm HO_2} + 2k_{12f}C_{\rm X}C_{\rm M_{12}}, \tag{18}$$

so that the low-temperature rates (14) are to be used if (18) is satisfied. The results are essentially independent of the value of $\varepsilon \ll 1$ utilized to measure the steady-state condition, provided that a sufficiently small value is employed.

Note that the above criterion requires two different conditions to be simultaneously satisfied, namely, that the temperature be below crossover, for $[(1+\varepsilon)k_{4f}C_{\rm M_4} - 2k_{1f}]$ to be positive with $\varepsilon \ll 1$, and that the H-atom concentration be above a given threshold value

$$C_{\rm H}^{*} = \frac{k_{6b}C_{\rm H_2}C_{\rm O_2} + k_{11f}C_{\rm H_2}C_{\rm HO_2} + 2k_{12f}C_{\rm X}C_{\rm M_{12}}}{[(1+\varepsilon)k_{4f}C_{\rm M_4} - 2k_{1f}]C_{\rm O_2}}. \tag{19}$$

In autoignition below crossover, the initial H-atom concentration is zero, so that the high-temperature rates (13) automatically are selected initially by this criterion, and, in fact, they reproduce the correct H rates that apply initially, prior to H achieving a steady state. Below crossover, the computed H-atom concentration increases with time and reaches the criterion (18) for use of the low-temperature chemistry, which then is employed until temperatures above crossover are reached. Direct use of (18) with $\varepsilon \ll 1$ thus is both better and computationally simpler than using the low-temperature rates (14) all the time below crossover although the predicted ignition times are only slightly different.

Figure 3 shows the evolution of the H radical during an autoignition process at an initial temperature of 800 K, well below crossover at atmospheric pressure, as obtained using detailed chemistry, and the three-step chemistry with hypothesized species

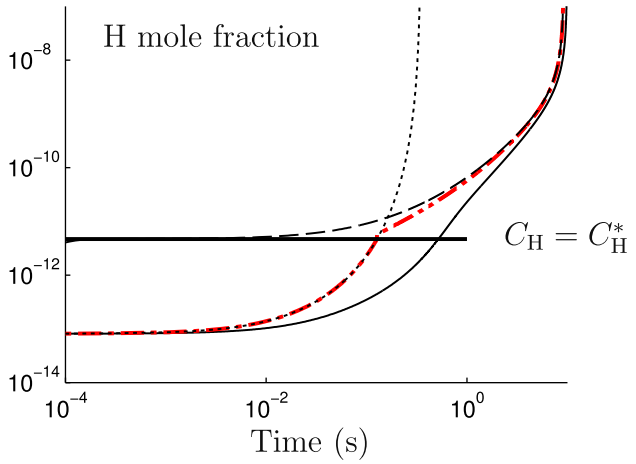

Fig. 3. The evolution with time of H mole fraction, in a homogeneous H_2–air mixture with $\phi = 1$ and $p = 1$ atm, initially at 800 K. The solid curve is the prediction using the detailed chemistry. The two sets of broken curves correspond to the three-step description using the rates $\omega^+_{\mathrm{I,\,II,\,III}}$ (dotted line), and $\omega^-_{\mathrm{I,\,II,\,III}}$ (dashed line). The dashed-dotted curve corresponds to the chemistry using both sets of rates, based on the criterion presented here, equivalent to switching when C_H reaches C^*_H, illustrated by the horizontal line.

X, using both sets of rates. It is seen from the detailed chemistry that there is a two-stage process, and during the first stage, the level of H is better predicted by the mechanism using the high-temperature set of rates, as stated above, since the H-atom steady state of the low-temperature process enforces a nonzero initial concentration C^*_H. This is because, for this period, HO_2 is key to the process, being a product of the only initiation step of importance: $H_2 + O_2 \rightarrow HO_2 + H$. The second stage, however, is not predicted by the high-temperature set of rates, which provoke an earlier ignition, by almost two orders of magnitude in this illustrative case. In that second stage, as indicated in [6], the process is better captured by putting H_2O_2 out of steady state, and HO_2 may be assumed to be in steady state, so that it is essential to use the low-temperature set of rates during this second stage.

We thus introduce here a hybrid three-step chemistry description, making use of the three overall steps involving H_2,O_2, H_2O, H and X, with the overall rates $\omega^+_{\mathrm{I,II,III}}$, where (18) is not satisfied and $\omega^-_{\mathrm{I,II,III}}$ where it is. Figure 3 includes the H evolution as obtained with this hybrid description: it shows that after HO_2 has played its role in the induction chemistry, allowing the H consumption rate to nearly reach its production rate, a smooth transition to the low-temperature set of rates is obtained, involving only a discontinuity in the slope, thereby correcting the early autoignition calculated using only the high-temperature set of rates.

Using such a criterion in choosing the appropriate set of rates for the three overall steps leads to continuous predictions of the variation of induction time with the initial temperature, with predictions being better than either one of the separate three-step descriptions. Figure 1 illustrates this point, showing the variation of the induction-time predictions with the detailed chemistry, with the two three-step descriptions (making exclusive use of either the high-temperature or the low-temperature sets of rates), and with the hybrid chemistry, the heavy dash-dotted curve. The gray bars show the period of time during which the low-temperature set of rates are used, that is, the hybrid description switches from using the high-temperature set of rates to the low-temperature set of rates at the bottom of the gray area. At the top end of the gray area the hybrid description switches back to using the high-temperature set of rates. It is seen that for each homogeneous ignition history, the computation starts with the high-temperature set of rates and continues to use them until H nearly reaches a steady state, which occurs shortly before the ignition time predicted by this set of rates. The low-temperature set of rates is then used until ignition, occupying most of the ignition time at low temperatures, but then when the temperature reaches the crossover temperature, the criterion automatically switches the high-temperature set of rates back on. As expected, the lower the temperature is, the more use is made of the low-temperature set of rates, so that induction times are predicted with reasonable accuracy over the whole range of temperature, making use of the best of each set of rates.

5. Representative predictions of the hybrid scheme

Figure 4 compares induction times of homogeneous mixtures as obtained with the detailed chemistry, the three-step hybrid description, and the four-step mechanism, for three different pressures and three different equivalence ratios. Comparison of induction times as obtained with the four-step mechanism and with the detailed chemistry show an outstanding agreement over the entire range of temperature, even in conditions close to crossover where the maximum differences in the predicted ignition time are close to 5%. The three-step hybrid scheme also leads to excellent predictions of induction times, with limited departures, up to 25–30% for conditions in the vicinity of crossover. However, the errors are less than 5% for temperatures above crossover, and less than 1% for temperatures sufficiently below. The agreement obtained by this hybrid procedure should be sufficient for most computational purposes.

Predictions for laminar premixed flames are indistinguishable from those included in Fig. 2 for both the 4-step and the 3-step hybrid descriptions, since they all reduce to the same two-step chemistry (10). The steady-state assumptions for HO_2 and H_2O_2 have, in fact, no effect on the laminar flame speed obtained with the reduced chemistries. For that same reason, computations of nonpremixed flames with the 4-step and the 3-step hybrid descriptions give results that are indistinguishable from those of the three-step reduced chemistry derived previously [4]. The accuracy of the reduced descriptions, with overpredictions of temperature on the order of 50 K for all strain rates in undiluted hydrogen–air counterflow flames at atmospheric pressure, as shown previously [4], is expected to improve at elevated pressure and also for diluted fuel feed, as can be inferred from the premixed-flame results of Fig. 2.

Figure 5 compares predictions of steady, planar detonation structure, reaching relatively high temperatures. Comparison of predictions with the detailed and corrected reduced chemistry, now using the high-temperature set of rates (13), shows that the degree of accuracy is quite satisfactory concerning the resulting induction length. These results are indistinguishable from those obtained with the four-step mechanism because the differences seen are associated with the absence of O and OH in these reduced mechanisms. Errors in peak radical concentrations in Fig. 5 are on the order of 20% and are due to the steady-state approximations for O and OH, there being little difference between predictions of the 12-step starting mechanism and the 21-step mechanism shown. Since O and OH are present at equilibrium in nonnegligible amounts, errors on the order of 5% appear in the final values of the temperature and pressure when these two species are not taken into account in the overall energy balance, as occurs when using the reduced chemistry. This is a well-known drawback of explicitly reduced chemistry: the selected subset of radicals has an impact in the evaluation of heat capacities, and thus on the thermodynamics, especially at high temperature where dissociations into radicals are of some quantitative importance. The Chapman–Jouguet conditions selected for the figure are those for the reduced chemistry, which differ little from those with detailed chemistry,

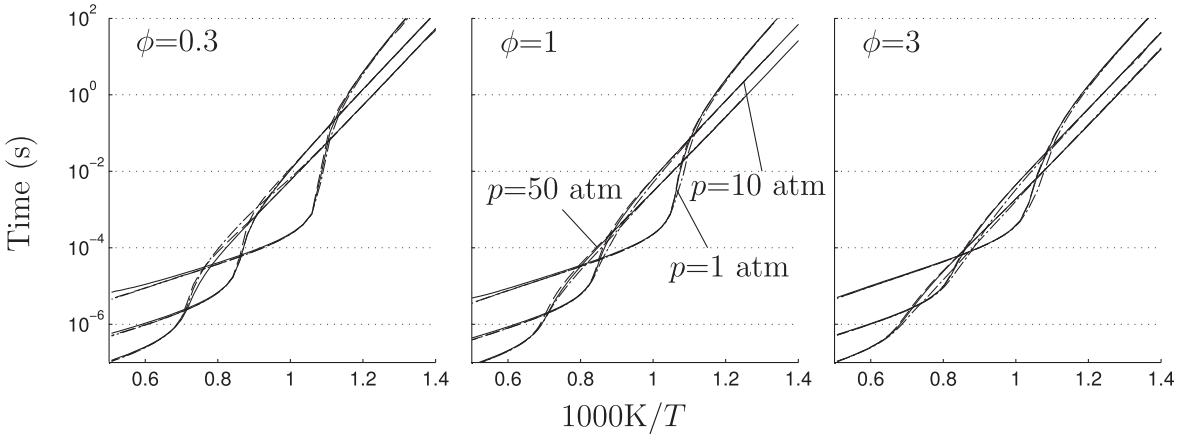

Fig. 4. The variation with initial temperature of the ignition time for three different pressures as obtained for a stoichiometric H_2–air mixture by numerical integration of the conservation equations with 21-step chemistry (solid curves) with the 4-step chemistry (dashed curves), and with the 3-step chemistry, making use of separate set of rates for high and low temperature autoignition (dashed-dotted curves).

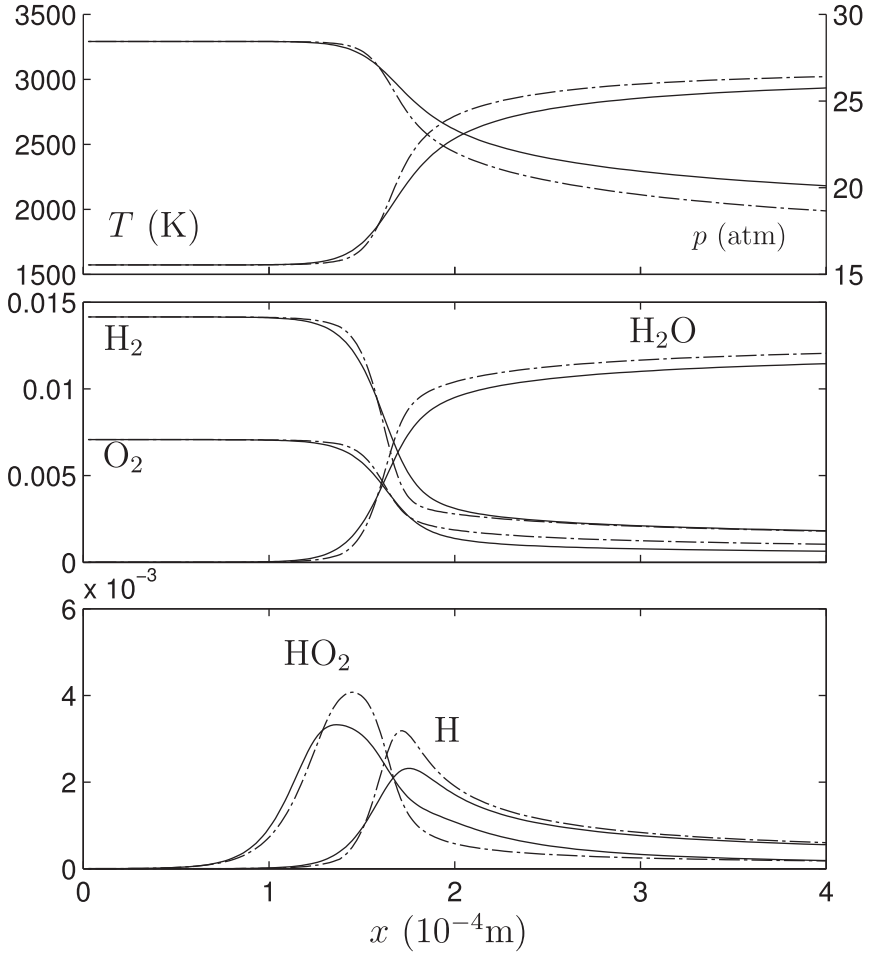

Fig. 5. The variation with the distance from the shock x of the pressure, temperature and species mole fractions in a Chapman–Jouguet detonation propagating in a stoichiometric hydrogen–air mixture with p = 1 atm and T = 300 K as obtained with the detailed 21-step chemistry (solid curves) and with the 3-step reduced mechanism with corrected rates (dash-dotted curves).

giving propagation velocities different by less than 2 m/s, both approximately being 2000 m/s. The results in this figure serve to test predictions for steady, planar, one-dimensional detonations, even though cellular detonations, with interacting high-pressure, high-temperature triple points encounter conditions for which the detailed chemistry fails, and vibrational relaxation need to be considered [12].

To improve any of these results, it would be necessary to reconsider the O and OH steady-state approximations, likely inconsistent with any three-step approximation.

Table 2
Computational times for an iteration in a 2D DNS with the detailed chemistry, the 4-step chemistry, and the 3-step chemistry, making use of separate sets of rates for high and low temperatures.

Scheme	Time (min)/iteration	Speed-up
Detailed chemistry	155	Reference
4-Step scheme	102	−34%
3-Step hybrid formulation	85	−45%

6. Comments on implementation and CPU efficiency

The most important aspect of chemistry reduction strategies, besides their accuracy, is the potential time saving for the user. Beyond the CPU efficiency, there are time losses associated with implementation complexity, as well as the time required for potential pre-processing (as in many tabulation methods, for example). The hybrid three-step formulation presented here has little complexity in the formulation since it only requires the implementation of the rates for the three reversible global steps. The corresponding routine (available from the first author on request) only requires as inputs the local composition and the local temperature and pressure. Since the formulation is of general applicability (for flames, detonations, and autoignition), no extra time is needed in checking its range of validity or in preparing a tabulation of the chemical rates. Last but not least, the CPU savings are substantial, even though this scheme only reduces the number of reactive species from 8 to 5. Table 2 illustrates the costs savings obtained for a 2D DNS computation of autoignition in a mixing layer, as in [13], making use of the NTMIX code [14]. The CPU savings in Table 2 are noticeable. Moreover, greater savings can be achieved in more chemistry-intensive simulations; trial computations in RANS-PDF contexts indicated a global speed-up over 75%.

There may be concerns about numerical problems arising from switching between Eqs. (13) and (14), in view of the resulting discontinuity in slope seen in Fig. 3. In this respect, it should be stated that no such problems were encountered in the 2-D simulations of Table 2. In addition, our previous 3-step formulation [4], which included reaction-rate modifications also keyed to a switch based on a steady-state criterion, was successfully tested and used in 3D LES computations of supersonic combustion [8], with a speed-up on the order of 20%, without numerical problems. Implementation of the present approach therefore appears to be problem-free.

7. Conclusions

In this paper, we have been looking for "universal" reduced chemistries for H_2–air combustion, which may be seen as the ultimate objective of our recent papers on H_2-oxidation reduced chemistry [4,6,8]. By universal, we mean reduced chemistries that may be used for computational purposes in all conditions of practical interest, including premixed and non-premixed combustion over the whole range of flammability, and also autoignition, whether the initial conditions place the system above or below the second explosion limit. Two options should be retained, which can find utility in different applications involving computation of flames and autoignition processes. For applications in which autoignition has to be reproduced with high fidelity, in conditions placing the system just below the second explosion limit, a four-step reduced chemistry, including H, HO_2 and H_2O_2 out of steady state should be retained, as being the only reduced description found to accurately describe autoignition in this regime. Autoignition-time predictions by the reduced chemistry are always better above the second explosion limit that just below.

From the four-step chemistry, two separate three-step reduced-chemistry descriptions were readily identified, having applicability for flames and autoignition in one of the two regimes (above or below the second explosion limit), but not qualifying as universal in the sense intended in this paper. A hybrid three-step reduced chemistry, making use of the best of these two mechanism, is, however, proposed, yielding reasonable accuracy for most conditions, with small departures of induction-time predictions from those with detailed chemistry at conditions very close to but below the second explosion limit. This three-step hybrid description was found to be accurate in premixed and non-premixed combustion, as well as in autoignition and planar detonation configurations, both above and below the second explosion limit. It is noteworthy that, with detailed chemistry, the five intermediates H, O, OH, HO_2, and H_2O_2 have to be included, while the hybrid description reduces this number to two, just H and X, an appreciable computational saving. Clearly, future derivations of multipurpose reduced mechanisms for syngas combustion including low-temperature autoignition could be based on the present development, thereby extending the applicability of previous reduced schemes [15].

Acknowledgements

This work was supported by the UE Marie Curie ITN MYPLANET, by the Spanish MCINN through Project # CSD2010-00010, by the Comunidad de Madrid through Project # S2009/ENE-1597, and by the US AFOSR Grant # FA9550-12-1-0138.

References

[1] F. Mauss, N. Peters, B. Rogg, F.A. Williams, in: N. Peters, B. Rogg (Eds.), Reduced Kinetic Mechanisms for Applications in Combustion Systems, Springer-Verlag, Heidelberg, 1993, pp. 29–43.
[2] Y. Ju, T. Niioka, Combust. Flame 99 (1994) 240–246.
[3] G. Balakrishnan, M.D. Smooke, F.A. Williams, Combust. Flame 102 (1995) 329–340.
[4] P. Boivin, C. Jiménez, A.L. Sánchez, F.A. Williams, Proc. Combust. Inst. 33 (2011) 517–523.
[5] C. Treviño, Prog. Astronaut. Aeronaut. 131 (1991) 19–43.
[6] P. Boivin, A.L. Sánchez, F.A. Williams, Combust. Flame 159 (2012) 748–752.
[7] P. Saxena, F.A. Williams, Combust. Flame 145 (2006) 316–323. <http://maemail.ucsd.edu/combustion/cermech>.
[8] P. Boivin, A. Dauptain, C. Jiménez, B. Cuenot, Combust. Flame 159 (2012) 1779–1790.
[9] D. Lee, S. Hochgreb, Int. J. Chem. Kinet. 30 (1998) 385–406.
[10] D. Fernández-Galisteo, A.L. Sánchez, A. Liñán, F.A. Williams, Combust. Flame 156 (2009) 985–996.
[11] D. Fernández-Galisteo, A.L. Sánchez, A. Liñán, F.A. Williams, Combust. Thor. Model. 13 (4) (2009) 741–761.
[12] B.D. Taylor, D.A. Kessler, V.N. Gamezo, E.S. Oran, Proc. Combust. Inst. 34 (2013). to appear.
[13] R. Knikker, A. Dauptain, B. Cuenot, T. Poinsot, Combust. Sci. Technol. 175 (2003) 1783–1806.
[14] M. Baum, T.J. Poinsot, D.C. Haworth, N. Darabiha, J. Fluid Mech. 281 (1994) 1–32.
[15] P. Boivin, C. Jiménez, A.L. Sánchez, F.A. Williams, Combust. Flame 158 (2011) 1059–1063.